Pergamon

Tetrahedron 58 (2002) 8863–8873

TETRAHEDRON

Gel formation properties of a uracil-appended cholesterol gelator and cooperative effects of the complementary nucleobases

Erwin Snip,[a] Kazuya Koumoto[a] and Seiji Shinkai[a,b,*]

[a]*Chemotransfiguration Project, Japan Science and Technology Corporation (JST), Kurume Research Center Bldg., 2432 Aikawa, Kurume, Fukuoka 839-0861, Japan*
[b]*Department of Chemistry and Biochemistry, Graduate School of Engineering, Kyushu University, Fukuoka 812-8581, Japan*

Received 21 June 2002; accepted 19 August 2002

Abstract—We designed and synthesized a uracil-appended cholesterol gelator (**1**) in order to control the gel stability and the gel morphology by addition of the complementary and non-complementary nucleobase derivatives. Compound **1** forms columnar stacks in cyclohexane due to the van der Waals interaction (cholesterol–cholesterol interaction) and the intergelator hydrogen bonding between uracil moieties. Addition of a 'monomeric' adenosine (**3**) into the gel only decreases the stability with increasing the concentration. The destabilization is ascribed to a lack of intergelator hydrogen bonding accompanied with forming the complementary base pairs between **1** and **3**. In contrast, addition of adenine-appended cholesterol (**7**) induces a different behavior; with increasing **7** concentration the mixed gel is initially stabilized and then destabilized, giving rise to a maximum at the ratio of **1**/**7**=1:1 for the T_{gel} plot. One may consider, therefore, that when the additive has a common, column-forming cholesterol moiety, the cholesterol–cholesterol interaction can operate cooperatively with the complementary base pairing. In addition, the gel fiber structure is clearly changed by the addition of **7**. Taking the fact that there is no report for such an additive effect inducing a structural change with maintaining the gel stability into consideration, our attempt combining cholesterol columnar stacks with the nucleobase additives provides a new methodology to control the stability and the morphology of organogels.

1. Introduction

Recently, considerable interest has been focused on the molecular self-assembly and the network formation by gelators, small organic molecules capable of gelling various solvents.[1] Through the self-assembly these molecules form one-dimensional fibrous aggregates, which can trap the solvent molecules. Gelators can be divided into two different categories, based on their intermolecular forces that enable them to form the network structure; that is, the forces used for the gel stabilization are hydrogen-bonding interactions,[2,3] van der Waals forces,[4] π–π stacking[5] and donor–acceptor interactions, etc.[6] In many cases, hydrogen bonding among gelator molecules plays an important role in the association processes. One example of this category is the sugar-based geletor.[3] Interestingly, a slight difference in the configuration of the hydroxyl groups results in quite different aggregation properties, which provide information useful for designing excellent gelators. Van der Waals forces, π–π stacking and donor–acceptor interactions, which are classified into the second category, are also important for the association of gelator molecules. It is well-known that these gelators tend to form tightly packed columnar stacks, which are considered to be the origin of the gel fiber formation. In particular, the cholesterol-based gelator is a typical example classified into this category. In many cases, the gel fibers exhibit a helical structure due to its inherent chirality.[4a,c,d] One may consider, therefore, that a cholesterol-based gelator appended to a functional group is an ideal building block to organize the functional groups in a helical fashion, whereby a stack of the cholesterol groups forms the central core and the functional groups appended are sticking outwards, like a spiral staircase, from this central helical column.[4a] When some additive which interacts with the functional group is added, the morphology and the stability of the gel would be readily affected by the additive. In fact, it was already found that addition of certain metals,[7,8] donor–acceptor molecules,[6] polymers,[9] etc.[10] does affect the morphology and the stability of the gel. It thus occurred to us that when some complementary (or non-complementary) nucleobase is added to the gel system, it should interact with the functional groups arranged around the helical column selectively to change the gelation properties.

To test this attractive working hypothesis, we initially designed and synthesized **1**.[11] Compound **1** is a cholesterol-based gelator which is functionalized by a uracil group as a

Keywords: supramolecular chemistry; organogel; cholesterol; nucleobase; complementary base pairing.

* Corresponding author. Address: Chemotransfiguration Project, Japan Science and Technology Corporation (JST), Kurume Research Center Bldg., 2432 Aikawa, Kurume, Fukuoka 839-0861, Japan. Tel.: +81-92-642-3583; fax: +81-92-642-3611; e-mail: seijitcm@mbox.nc.kyushu-u.ac.jp

0040–4020/02/$ - see front matter
PII: S0040-4020(02)01059-1

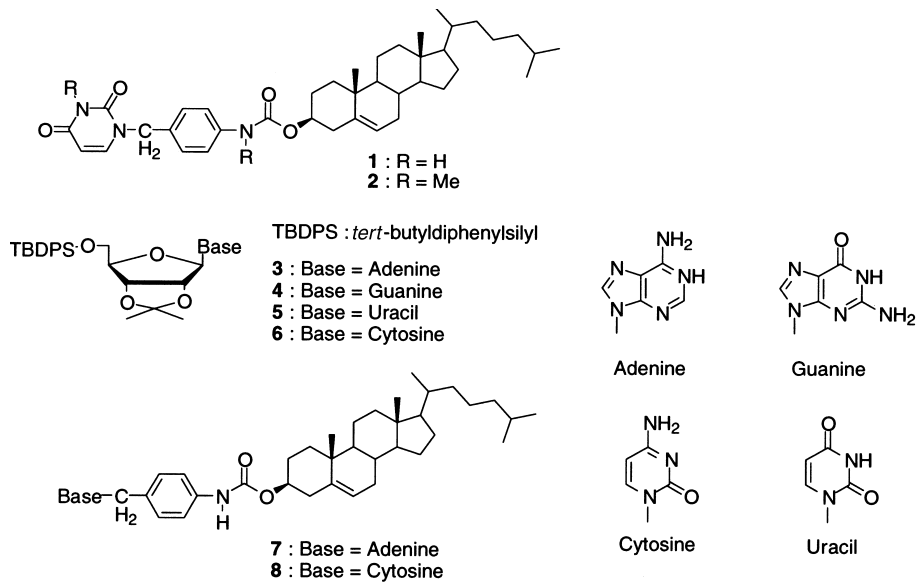

recognition site. One may expect, therefore, that when the gel-forming cholesterol moieties aggregate into a one-dimensional stack,[4a] the uracil moieties are, expectedly, chirally arranged around the columnar structure. This aggregation mode may show some character like poly(U). In this context, it is particularly intriguing to know what happens when the complementary adenine derivative is added. In this full paper,[11] we not only examine the gelation properties of **1** and **2** thoroughly but also assess the influence of **3**–**8** on the gel stability. One can expect that **3**–**6** without a cholesterol group would be bound onto the columnar aggregate, reflecting the complementary or non-complementary relationship, whereas **7**, **8** with a cholesterol group would be bound into the columnar aggregate due to the cholesterol–cholesterol interaction. We consider that this structural difference, which should appear as the difference in the gel stability, is useful to systematically understand the mechanism of the organogel formation.

2. Results and discussion

The synthesis of compound **1** was achieved in four steps (Scheme 1): bis-silylation of uracil with hexamethyldisilazane (HMDS) was followed by alkylation of *N*1 of uracil with 4-nitrobenzyl bromide according to the method of

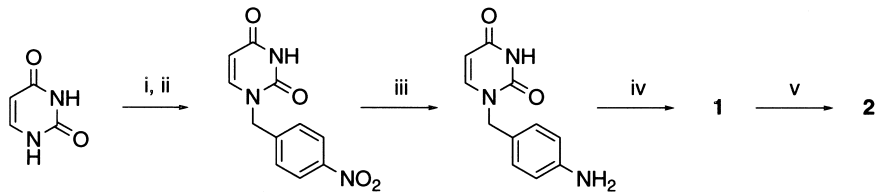

Scheme 1. Syntheses of uridine-based cholesterol gelators. *Reagents and conditions*: (i) HMDS, $(NH_4)_2SO_4$, reflux; (ii) 4-nitrobenzyl bromide, acetonitrile, reflux; (iii) $SnCl_2$, EtOH, 70°C; (iv) cholesteryl chloroformate, NEt_3, THF–pyridine, rt; (v) NaH, MeI, DMF, rt.

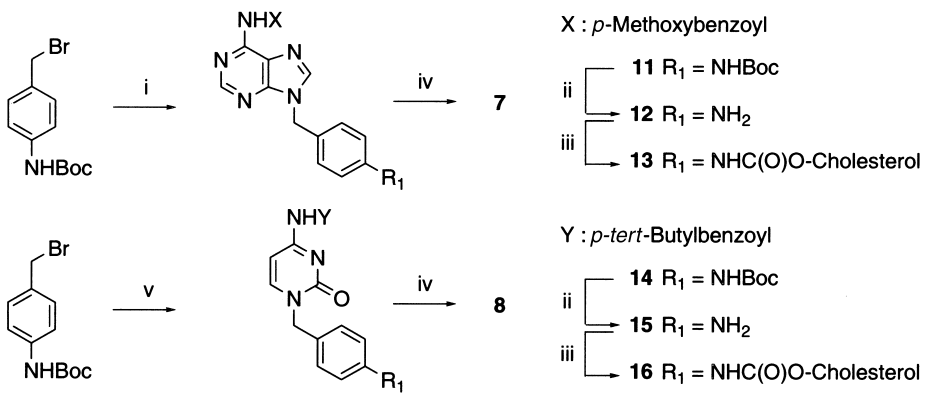

Scheme 2. Syntheses of adenine and cytosine-based cholestrol geletors. *Reagents and conditions*: (i) NaH, 6-anisoyladenine, DMF, rt; (ii) TFA, rt; (iii) cholesteryl chloroformate, NEt_3, THF, rt; (iv) 25% NH_3 aqueous solution, THF, 50°C; (v) NaH, 4-*tert*-butylbenzoylcytosine, DMF, rt.

Table 1. Gelation for **1**

Solvent	[**1**] (wt%)	Result
n-Hexane*	3/1	I/I
n-Octane*	3/1	I/G_p
Cyclohexane*	3/1	G/G
Benzene*	3/1	G/S
Toluene*	3/1	G/S
p-Xylene*	3/1	G/S
Diethyl ether*	3/1	I/I
Ethyl acetate*	3	P
Acetone*	3	P
Acetonitrile*	3/1	I/P
Dichloromethane*	3	S
Chloroform	3	S
Methanol*	3	P
Ethanol*	3	P
n-Butanol*	3/1	G/S
Octanol*	3/1	P/S
Water	3	P
Decalin*	3/1	G/S

Results: G=gel; G_p=partial gel; P=precipitation; S=solution; I=insoluble. Solvents marked with * have been dried over molecular sieve 4 Å.

Robins and Hatfield.[12] After reduction of the nitro group with tin(II) chloride,[13] the resulting amine was reacted with cholesteryl chloroformate to yield compound **1**. The methylated derivative **2** was synthesized by methylation of **1** with MeI and NaH.

Nucleoside derivatives (**3**–**6**) were synthesized according to the reported method.[14] Synthesis of compounds **7** and **8** was carried out in a similar way to that of **1** (Scheme 2). The Boc-protected 4-aminobenzyl bromide was used to alkylate *N*6-anisyladenine and *N*4-*tert*-butylbenzoylcytosine.[15] Deprotection of the Boc group of **11** and **14** was carried out by treatment with TFA. The resulting amines (**12** and **15**) were reacted with cholesteryl chloroformate. The deprotection to yield the nucleobases **7** and **8** was achieved by treatment with aqueous ammonia at 50°C.

As shown in Table 1, solvents which are gelated by compound **1** (3 wt%) were *n*-octane, cyclohexane, benzene, toluene, *p*-xylene, *n*-butanol and decalin.[8] Only cyclohexane is gelated by **1** at 1 wt%. Therefore, cyclohexane was chosen as the standard solvent for the subsequent studies. The reference compound **2** can also gelate cyclohexane above 0.6 wt%. Next, we estimated the gel stability difference between **1** and **2** by comparing the gelation temperatures (T_{gel}). The T_{gel} values were determined at the various gelator concentrations. The minimum gelation concentration (MGC) to form a gel was estimated to be 0.25 wt% for **1**, 0.6 wt% for **2**, respectively. It is seen from Fig. 1 that **1** is capable of producing the very stable gel; when the T_{gel} values were evaluated in a sealed tube, they were even higher than the boiling point of cyclohexane (bp=80.7°C). On the other hand, the T_{gel} values for **2** were lower by about 60°C than those for **1**, even though the gelator concentrations used for **2** were much higher than those used for **1**. The results clearly support the view that the **1** gels are stabilized by the hydrogen bonding including the one or two NH groups, which are lost in **2** by methylation. In fact, when we measured ^{1}H NMR spectroscopy in $CDCl_3$ as a function of the gelator concentration, both NH signals (carbamate; N1 and uracil; N2) were shifted to lower magnetic field with the increase in the gelator concentration (Table 2). The finding indicates that the NH bonds play an important role in forming intermolecular hydrogen bonds. In particular, the $\Delta\delta$ of N2 is much larger than that of N1. The fact implies that both NH protons contribute to the gelator–gelator hydrogen-bonding interaction and judging from the magnitude of their chemical shifts, N2 should play a bigger role.

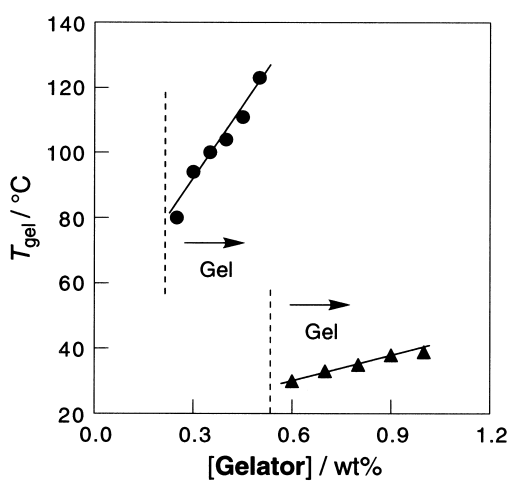

Figure 1. Plots of T_{gel} against geletor concentrations in cyclohexane. Dashed line shows MGC: **1** (●), **2** (▲).

Table 2. Chemical shifts of the carbamate–NH (indicated as N1) and the uracil–NH (N2) of **1** at different concentrations in $CDCl_3$

[**1**] (mmol dm^{-3})	δ_{N1} (ppm)	δ_{N2} (ppm)
3.17	6.592	8.056
15.7	6.685 (+0.093)	8.506 (+0.450)
31.7	6.771 (+0.179)	8.825 (+0.769)

In order to obtain a deeper insight into the aggregation mode, circular dichroism (CD) spectroscopy was used to monitor the gel to sol phase transition. The CD spectra of a gelated sample of **1** (4.13 mmol dm^{-3}, 0.25 wt%) and of **2** (9.13 mmol dm^{-3}, 0.6 wt%) were recorded at various temperatures. The molar ellipticities at the absorption maximum (260 nm for **1** and 257 nm for **2**) plotted against temperature are shown in Figs. 2(a) and (b), respectively. In Fig. 2(a), one can observe a drastic decrease in the CD intensity between 78 and 81°C, which can be ascribed to a gel to sol transition. This temperature is in perfect agreement with the T_{gel} measured under the same concentration (see Fig. 1). In addition, we noticed that the sample is still CD-active even above 81°C, although the intensity is much weaker than that below 81°C. This shows that oligomeric molecular aggregates still exist above the T_{gel} although they are not so stable as to gelate the solvent. For compound **2**, a phase transition was observed at around 26°C (Fig. 2(b)), which is also in good agreement with the T_{gel} of **2**. It is worthy to mention, however, that the sample becomes totally CD-silent above the T_{gel}. This suggests that **2** without the NH group is discretely dissolved in the sol solution.

We also compared the shape of the CD spectra for **1** and **2** above and below the T_{gel} (Fig. 3). As mentioned above, the CD spectral shape for **1** is similar between the sol phase and

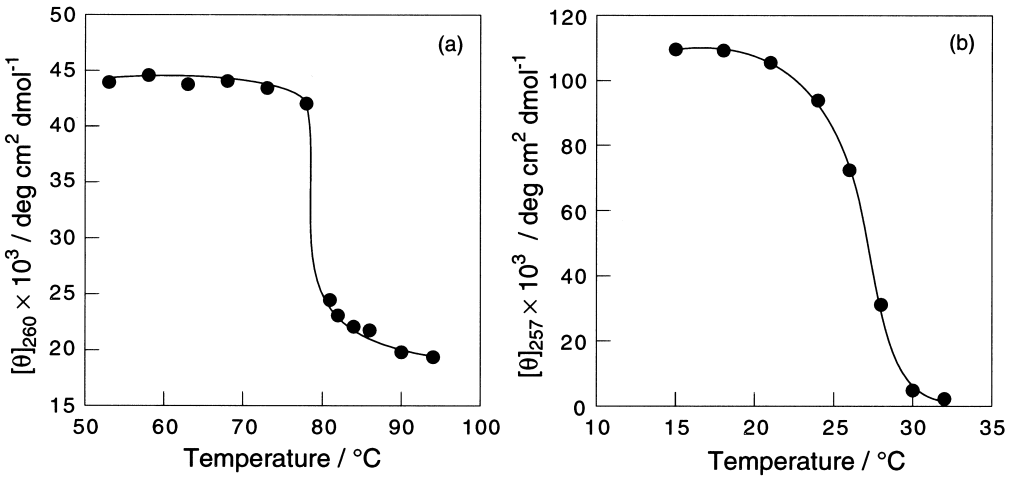

Figure 2. Plots of $[\theta]_{\lambda max}$ against temperature for **1** (a) and for **2** (b): [**1**]=4.13 mmol dm^{-3} (0.25 wt%) and [**2**]=9.13 mmol dm^{-3} (0.6 wt%) in cyclohexane.

the gel phase, and the gel phase gives the stronger CD intensity (λ_{max} 259.6 nm, λ_{min} 235.8 nm). The finding suggests that the oligomeric aggregates already exist in the sol phase, which eventually grow up to the fibrous aggregates in the gel phase. Further surprising is the finding that the CD spectrum of **1** is quite similar to that of poly(uridylic acid) (poly(U)).[16] This implies that the uracil moieties in compound **1** are arranged in an ordered helical fashion which is similar to that in poly(U). On the other hand, **2** is totally CD-silent in the sol phase but becomes CD-active only in the gel phase. Judging from the complex CD spectral pattern, it seems to be a mixture of a few different CD spectra. In **2**, there is no hydrogen-bonding site which can govern the molecular packing mode, and the residual driving force for aggregation is the van der Waals interaction which is classified, more or less, into the non-directional force. This situation would allow **2** to result in a few different aggregation modes. We now consider that this character is compatible with the fact that the organogel system features polymorphism.[1–4]

To substantiate this difference between **1** and **2** from a visual insight, scanning electron microscopy (SEM) pictures of the xerogels prepared from **1** and **2** in cyclohexane were taken (Fig. 4). For both xerogels one can recognize a well-developed network structure consisting of fibrils. Compared Fig. 4(a) with Fig. 4(b), the diameter and the detailed structure are different. For compound **1**, the diameter of the fibrils is about 20–40 nm and the fiber structure shows the clear right-handed helicitiy. On the other hand, the diameter of compound **2** is about 70–160 nm, which is 3–4 times larger than that of **1** and no helical motif is observed. These results consistently support the view that the hydrogen-bonding interaction plays a central role to create a neat molecular packing in the gel phase, which leads to the helical superstructure and the strong CD intensity, reflecting the molecular chirality. Here, it becomes very intriguing to assess what is induced by the addition of complementary or non-complementary nucleobase derivatives.

First, we examined the influence of added nucleoside derivatives (**3**–**6**). If these derivatives enlarge the π-area by the hydrogen-bonding interaction and increase the π–π stacking ability, then the addition would stabilize the gel system.[16] In contrast, if these derivatives efficiently cleave the intergelator hydrogen bonds which contribute to the gel stabilization, then the addition would destabilize the gel system. To clarify the additive effect, we measured the T_{gel} values of **1** as a function of added **3**–**6** concentrations. As shown in Fig. 5, the addition of **4**–**6** induces a drastic

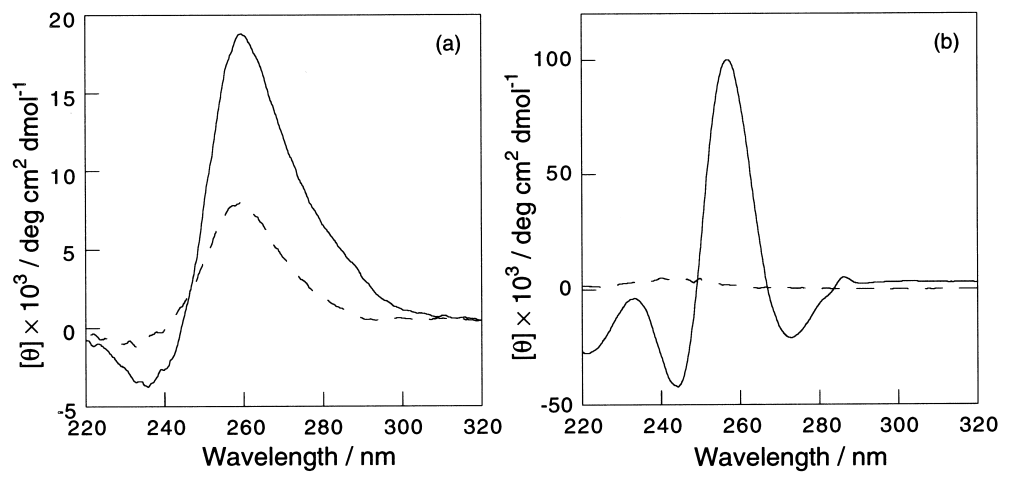

Figure 3. CD spectra of **1** (a) and **2** (b) below and above T_{gel}. Solid line shows the CD spectra below T_{gel} and dashed line shows that above T_{gel}: [**1**]=4.13 mmol dm^{-3} and [**2**]=9.13 mmol dm^{-3}.

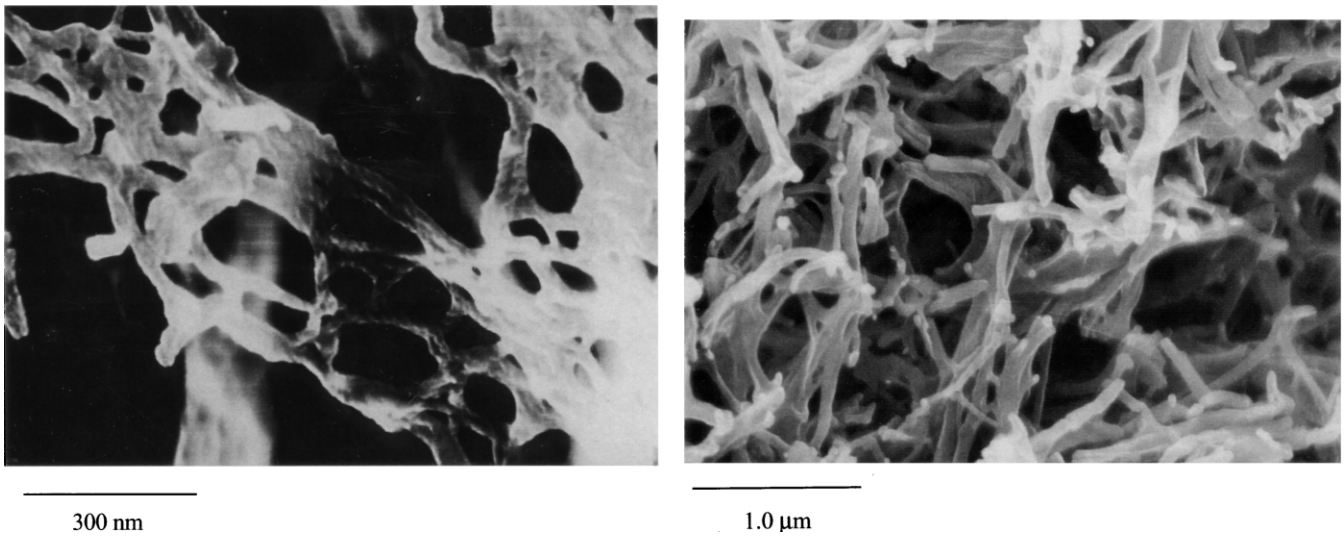

Figure 4. SEM picture of the xerogel prepared from **1** (a) and **2** (b) in cyclohexane.

decrease in the T_{gel} values. In particular, **4** bearing a guanosine moiety exerted the largest destabilization effect: the addition of only 0.01 equiv. of **4** lower the T_{gel} from 123 to 31°C and the gel disappeared above 0.05 equiv. of **4**.

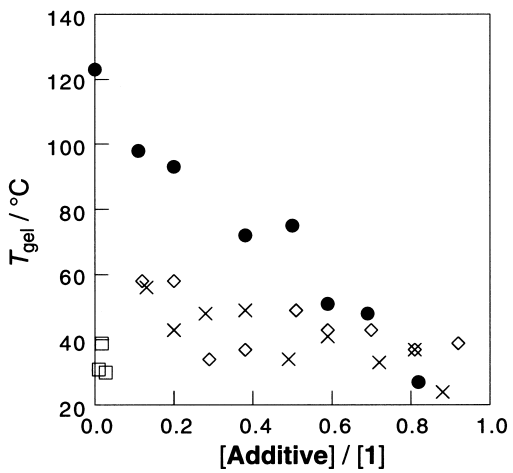

Figure 5. T_{gel} of gels formed from **1** (7.94 mmol dm^{-3}) in cyclohexane plotted against additive concentrations: **3** (●), **4** (□), **5** (×) and **6** (◇).

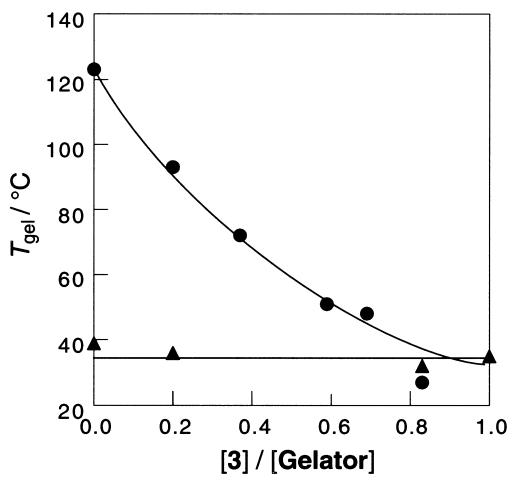

Figure 6. Influence of added **3** on of the T_{gel} for **1** (●) and for **2** (▲).

Compound **4** has the three hydrogen-bonding donor–acceptor sites and the π-area is larger than those of **5** and **6**. Presumably, **4** is strongly bound to the fibrous aggregate of **1**, disordering the intergelator hydrogen-bonding and π–π stacking interactions. In contrast, **3** bearing an adenosine moiety complementary to the uracil moiety in **1** showed a mild destabilization effect, relative to **4**–**6**. We consider, therefore, that in the **1**+**3** system the destabilization effect arising from the hydrogen-bond cleavage is partially compensated by the stabilization effect of the π–π stacking among the π-systems enlarged by base pairing.[16]

In order to confirm that the T_{gel} decrease is mainly due to the hydrogen-bond cleavage, we compared the influence of the additives on the T_{gel} values of **1** and **2**. Compound **2** should be less affected by addition of **3** because its hydrogen bonding site is lost by methylation. As can be seen in Fig. 6, there is no T_{gel} decrease for the **2**+**3** system. It is undoubted, therefore, that the **1** gel is stabilized by the intergelator hydrogen-bonding interaction, like the uracil–uracil hydrogen-bonding interaction in poly(U)[17] but destabilized by the competitive hydrogen-bond formation with additives. We also measured ^{1}H NMR spectra of **1** in the presence of **3**, the results being summarized in Table 3. Addition of **3** induces the downfield shift of only the peak assignable to N2 (uracil–NH), supporting the view that the adenine moiety of **3** forms the selective hydrogen bonds with the uracil moiety of **1**.

The foregoing findings prompted us to synthesize compound **7** bearing both a cholesterol moiety and an adenine moiety. One can expect that the cholesterol moiety would

Table 3. Chemical shifts of the carbamate–NH (indicated as N1) and the uracil–NH (N2) of **1** in the absence and the presence of **6**

Molar ratio [**3**]/[**1**]	δ_{N1} (ppm)	δ_{N2} (ppm)
0	6.592	8.056
1.0	6.602 (+0.010)	8.576 (+0.520)
2.0	6.609 (+0.017)	8.907 (+0.851)

Measurement conditions: [**1**]=2.85 mmol dm^{-3} in $CDCl_3$ at room temperature. TMS was used as internal standard.

Table 4. Gelation tests of nucleobase gelators in cyclohexane

[Gelator] (wt%)	Phase		
	1	**7**	**8**
0.25	G	P	I
0.50	G	P	I
1.00	G	P	I
2.00	G	I	I

Results: P=precipitation, G=gel, I=insoluble.

form a columnar stack with that in **1** and the adenine moiety would form complementary hydrogen bonds with the uracil moiety in **1**. We also synthesized compound **8** bearing a cholesterol moiety and a cytosine moiety for comparison. Before mixing **1** with **7** or **8**, the gelation ability of **7** and **8** was estimated in cyclohexane. As shown in Table 4, neither **7** nor **8** was able to form a gel. Then, we tested the gelation ability of mixtures of **1**+**7** and **1**+**8**. It is seen from Table 5 that only the **1**+**7** mixture can act cooperatively in the gel formation. On the other hand, the mixing of **1** with **8** bearing a non-complementary cytosine moiety simply resulted in the precipitate. To substantiate the importance of the complementarity the T_{gel} values for the **1**+**7** mixture were measured at different **1**/**7** ratios. The results are plotted in Fig. 7. Very interestingly, the **1**+**7** mixture gave a maximum T_{gel} value at **1**/**7**=1:1 ratio. This characteristic feature is related to both the complementary base pairing and the cholesterol–cholesterol interaction between the gelator (**1**) and the complementary additive (**7**).

We measured the IR spectra of the **1**+**7** mixture to substantiate the suggested base pair formation between the uracil moiety of **1** and the adenine moiety of **7**. IR spectroscopy is known to be a useful tool in proving the presence of the hydrogen bonding in the helix and duplex formation in polynucleotides. The frequencies of diagnostic peaks are listed in Table 6. The IR spectrum of **7** has only one carbonyl peak, which appears at the same frequency as that in **1**, namely at 1710 cm^{-1}. Therefore, this carbonyl peak is assigned to the carbamate group whereas other two carbonyl peaks of **1** are assigned to those in the uracil moiety. The duplex formation of poly(U) and poly(A) was studied by IR spectroscopy previously.[17] Analogously to the poly(U)+poly(A) polynucleotide system, the **1**+**7** gel system shows that one carbonyl stretching peak (1645 cm^{-1}) disappears and another peak at 1685 cm^{-1} remains. These results clearly prove the complementary hydrogen-bond formation between the uracil moiety of **1** and the adenine moiety of **7**.

Table 5. Gelation tests for mixtures of **1**+**7** and **1**+**8**

Molar ratio [**7**]/[**1**]	[**7**] (wt%)			
	0.15	0.25	0.50	1.00
1.00	S	S	G	G
Molar ratio [**8**]/[**1**]	[**8**] (wt%)			
	0.15	0.25	0.50	1.00
0.65	I	I	I	I
1.00	I	I	I	I
Molar ratio [**7**]/[**8**]	[**8**] (wt%)			
	0.15	0.25	0.50	1.00
0.50	I	I	I	I
1.00	I	I	I	I
1.50	I	I	I	I

Results: S=solution, G=gel, I=insoluble.

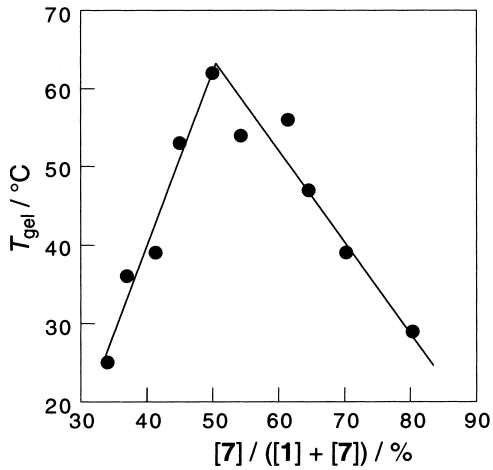

Figure 7. T_{gel} for the **1**+**7** mixtures of **1** and **7** in cyclohexane plotted against the molar ratio of **7**.

Table 6. Characteristic FT-IR bands in solutions and a gel

Gelator[a]	Solvent (state)	$\nu_{C=O}$ (cm^{-1})
1	$CDCl_3$ (sol)	1710, 1685, 1645
7	$CDCl_3$ (sol)	1710
1+**7**	Cyclohexane (gel)	1730,[b] 1685

[a] Concentration of the gelators was kept constant. [**1**]=[**7**]=0.25 wt% or 4.13 mmol dm^{-3}.
[b] The peak was observed as a shoulder.

We also measured the CD spectrum of the **1**+**7** mixture in order to investigate the possible structural change induced by added **7** (Fig. 8). The **1**+**7** mixture shows an exciton-coupling-type CD band at shorter wavelength region (λ_{max} 230.2 nm, λ_{min} 246.6 nm). This spectral pattern is different from that of the poly(U)+poly(A) mixture (λ_{max} 270.6 nm, λ_{min} 245.8 nm) which is more or less similar to that of poly(U) itself (λ_{max} 263.4 nm, λ_{min} 244.8 nm).[18] The poly(U)+poly(A) mixture enjoys the Watson–Crick-type

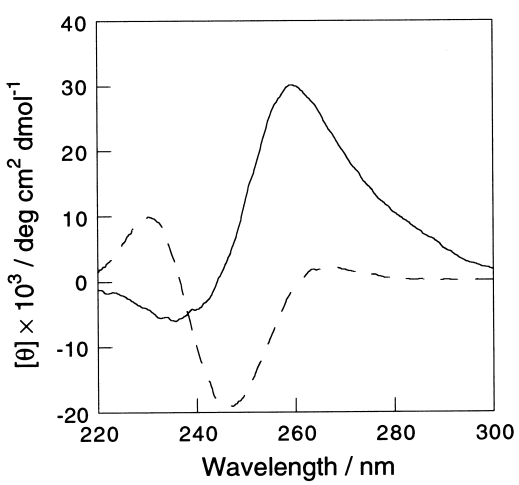

Figure 8. Comparison of the CD spectra of **1** in the absence (solid line) and the presence of **7** (dashed line).

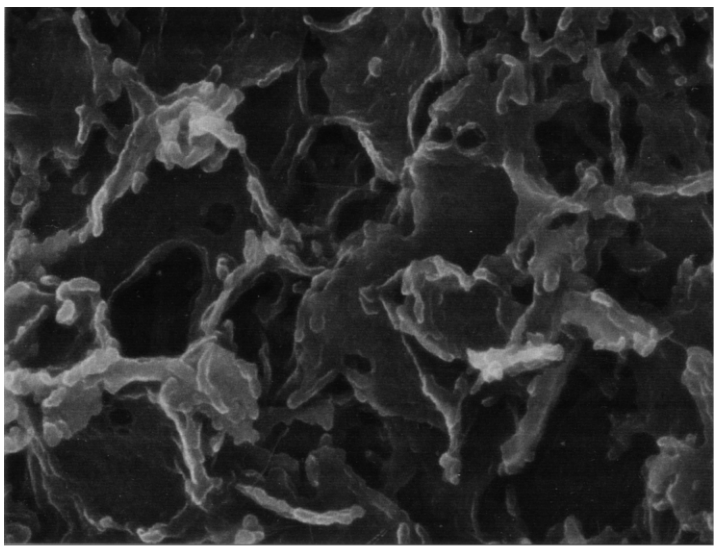

Figure 9. SEM picture of the xerogel prepared from the equimolar **1**+**7** mixture: [**1**]=[**7**]=1.0 wt%.

edge-to-edge hydrogen-bonding interaction.[19] In the **1**+**7** mixture, on the other hand, this type of interaction is rather difficult when they use the cholesterol moieties as a common skeleton to form a central columnar stack. We now consider, therefore, that **1** and **7** utilize some complementary interaction, which is different from the typical Watson–Crick-type one.

Fig. 9 shows a typical SEM picture of the xerogel obtained from the **1**+**7** mixture at 1:1 ratio. Interestingly, one can recognize that the xerogel shows a mixture of both sheet and fiber structures. In addition, the fiber structure with the diameter of 30–60 nm grows up at the edge of the sheet structure. The size is comparable with that of **1**, but the helical motif is not observed clearly. Although we cannot further clarify the detailed structural transition, this feature is quite interesting because to induce the morphological transition in the gelator system is usually very difficult. From this viewpoint, our attempt using the cholesterol gelator can be considered to be very fruitful.

3. Conclusion

In this paper, we designed and synthesized a uracil-appended cholesterol gelator in order to control the morphology and the stability by addition of the complementary nucleobase derivatives. Our first attempt was to use nucleoside derivatives as binding sites. The NMR analyses revealed that although compound **3** can interact with the uracil moiety, it only decreases the gel stability. In contrast, addition of cholesterol appended adenine (**7**) rather enhances the gel stability. This difference is ascribed to the contribution of the ditopic hydrogen-bonding and van der Waals interactions. Namely, the new stabilization effect arising from the van der Waals interaction compensates the destabilization arising from the loss of the intergelator hydrogen bonding. Although the studies on organogels are now rapidly expanding, it is still difficult to design a gelator system whose morphology and stability can be controlled as desired. We believe that our strategy using the complementary additives provides a new methodology to control the morphology and the stability in the gel system.

4. Experimental

4.1. General remarks

All reagents were used without further purification and all solvents were used after purification by distillation. ^{1}H and ^{13}C NMR spectra were measured with a Brucker ARX-300 spectrometer using tetramethylsilane as an internal standard. Infrared spectra were recorded with a SHIMADZU FT-IR 8100M spectrometer. The SIMS measurements were carried out in a glycerol or 3-nitrobenzyl alchol matrix with xenon as a primary ion.

4.1.1. 1-(4-Nitrobenzyl)uracil (9). To a suspension of uracil (1.67 g, 15 mmol) in hexamethyldisilazane (50 mL) a catalytic amount of ammonium sulfate was added. This was refluxed for 16 h during which the mixture turned into a clear solution. The volatiles were removed in vacuo. A portion of this silylated uracil (1.00 g, 3.9 mmol) was dissolved in acetonitrile (40 mL) and cooled with an ice bath. A solution of 4-nitrobenzylbromide (421 mg, 2.0 mmol) in acetonitrile (10 mL) was added. The mixture was refluxed for 24 h, after which the reaction was nearly complete (TLC, MeOH–$CHCl_3$=1:4, R_f (product)=0.48). The volatiles were removed in vacuo and the residue was extracted with MeOH–$CHCl_3$ (1:4, 50 mL). The filtrate was adsorbed onto silica and flash column chromatography (MeOH–$CHCl_3$ 1:9) yielded the title compound (231 mg, 48%). An analytically pure sample was obtained by recrystallisation from MeOH. Mp 240–242°C (lit.[4] 225°C). IR (KBr) ν_{max} (cm^{-1}) 3425 (w, N–H), 3154, 3096 and 3020 (m, Ar-H), 2882 and 2839 (m, CH_2), 1690 and 1670 (s, C=O), 1514 and 1348 (NO_2), 856 (C–NO_2);

^{1}H NMR (300 MHz, DMSO-d_6, TMS, 25°C): δ (ppm) 11.40 (1H, s, N*H*), 8.22 (d, ^3J(H,H)=8 Hz, 2H, Ar-H), 7.80 (dd, ^3J(H,H)=8, 0.9 Hz, 1H, H_6), 7.35 (d, ^3J(H,H)=8 Hz, 2H, Ar-H), 5.64 (dd, ^3J(H,H)=8, 1 Hz, 1H, H_5), 5.00 (s, 2H, CH_2); MS (SIMS): *m/z*: 248 $[MH]^+$; elemental analysis calcd (%) for $C_{11}H_9N_3O_4$ (247.2): C 53.44, H 3.67, N 17.00; found C 53.48, H 3.65, N 17.05.

4.1.2. 1-(4-Aminobenzyl)uracil (10). Tin(II) chloride dihydrate (958 mg, 4.3 mmol) was added to a suspension of 1-(4-nitrobenzyl)uracil (**9**) (210 mg, 0.8 mmol) in ethanol (4 mL). After heating to 70°C for 2 h, TLC (MeOH–$CHCl_3$ 1:9) showed that the reaction was complete. The solution was allowed to reach room temperature and was subsequently poured into ice water (20 mL). Sodium bicarbonate (saturated solution) was added till the solution became pH 8, followed by extraction with $CHCl_3$. The combined organic layers (180 mL) were washed with brine (75 mL) and dried over magnesium sulfate. Evaporation of the solvent in vacuo yielded the title compound (140 mg, 78%). An analytically pure sample was obtained by recrystallisation from MeOH, mp 235–237°C. IR(KBr) ν_{max} (cm^{-1}) 3465 (m, N–H), 3370 (s, N–H), 3168, 3104 and 3036 (m, Ar-H), 2828 (w, CH_2), 1700 and 1675 (s, C=O); ^{1}H NMR (300 MHz, DMSO-d_6, TMS, 25°C): δ (ppm) 11.24 (1H, s, N*H*), 7.65 (1H, d, *J*=7.8 Hz, H_6), 6.98 (2H, d, *J*=8.4 Hz, Ar-*H*), 6.50 (2H, d, *J*=7.7 Hz, Ar-*H*), 5.53 (1H, d, *J*=8.1 Hz, H_5), 5.11 (2H, s, NH_2), 4.64 (2H, s, CH_2); MS (SIMS): *m/z*: 218 $[MH]^+$, 217 $[M]^+$; elemental analysis calcd (%) for $C_{11}H_{11}N_3O_2$ (217.2): C 60.82, H 5.10, N 19.34; found C 60.68, H 5.61, N 19.25.

4.1.3. 1-(4-(Cholesterylcarbonylamino)benzyl)uracil (1). Cholesteryl chloroformate (357 mg, 0.8 mmol) dissolved in THF (4 mL) was added dropwise to a suspension of 1-(4-aminobenzyl)uracil (**10**) (144 mg, 0.7 mmol) and triethylamine (0.17 mL, 1.2 mmol) in THF (3 mL). After stirring for 3 h, CH_2Cl_2 and water were added, the organic layer was separated, washed with brine and dried over magnesium sulfate. The solvents were removed in vacuo and subsequent flash column chromatography (silica; CH_2Cl_2–acetone 4:1) yielded the title compound as a white solid (220 mg, 53%), mp 243–245°C; IR(KBr) ν_{max} (cm^{-1}) 3441 and 3343 (w, N–H), 3196 and 3054 (w, Ar-H), 2948, 2905 and 2851 (m, alkyl-H), 1682 and 1680 (s, C=O), 1225 (s, C–O); ^{1}H NMR (300 MHz, $CDCl_3$, TMS, 25°C): δ (ppm) 8.65 (1H, s, N*H*), 7.40 (2H, d, *J*=8.4 Hz, Ar-*H*), 7.24 (2H, d, *J*=8.7 Hz, Ar-*H*), 7.14 (1H, d, *J*=7.8 Hz, H_6 uracil), 6.73 (1H, s, N*H*), 5.68 (1H, d, *J*=7.8 Hz, H_5 uracil), 5.40 (1H, d, *J*=5.1 Hz, H_6 cholesteryl), 4.85 (2H, s, benzyl CH_2), 4.61 (1H, m, OC*H* cholesteryl), 2.39, 1.91 and 1.64–0.85 (43H, m, cholesteryl-*H*); MS (SIMS): *m/z*: 629 $[M-H]^-$, 628 $[M-2H]^-$, 517 [M−uracil−H]$^-$, 111 [uracil−H]$^-$; elemental analysis calcd (%) for $C_{39}H_{55}N_3O_4$ (629.9): C 74.37, H 8.80, N 6.67; found C 73.95, H 8.72, N 6.57.

4.1.4. 1-(4-(Cholesterylcarbonylmethylamino)benzyl)-3-methyluracil (2). Sodium hydride (23 mg, 1.0 mmol) was added to solution of 1-(4-(cholesterylcarbonylamino)-benzyl)uracil (**1**) (60 mg, 95 μmol) in DMF (4 mL). After stirring for 5 min, methyl iodide (24 μL) was added. After 3 h, the reaction mixture was cooled to 0°C and a few drops of water were added. Cooling was stopped and more water and CH_2Cl_2 were added. The organic layer was separated and the water layer was extracted twice with CH_2Cl_2. The combined organic layers were washed with brine and dried over magnesium sulfate. The solvent was removed in vacuo and subsequent preparative thin layer chromatography (silica; CH_2Cl_2–acetone 9:1) yielded the title compound as a white solid (42 mg, 67%). An analytically pure sample was obtained by recrystallisation from MeOH. Mp 162–163°C; ^{1}H NMR (300 MHz, $CDCl_3$, TMS, 25°C): δ (ppm) 7.26 (4H, m, Ar*H*), 7.17 (1H, d, *J*=8.1 Hz, H_6), 5.76 (1H, d, *J*=7.8 Hz, H_5), 5.37 (1H, d, *J*=5.1 Hz, H_6 cholesteryl), 4.92 (2H, s, CH_2), 4.56 (1H, m, OC*H*-cholesteryl), 3.37 (3H, s, NCH_3) 3.29 (3H, s, NCH_3), 2.36, 1.90, 1.63–0.85, 0.67 (43H, m, cholesteryl-*H*); MS (SIMS): *m/z*: 656 $[M-H]^-$, 655 $[M-2H]^-$; elemental analysis calcd (%) for $C_{41}H_{59}N_3O_4$ (657.9): C 74.85, H 9.04, N 6.39; found C 74.88, H 9.08, N 6.38.

4.1.5. 2′,3′-*O*-Isopropylidene-5′-*O*-(2-methylpropyl)diphenylsilyl-adenosine (3). (2-Methylpropyl)diphenylchlorosilane (0.3 mL, 1.2 mmol) was added to a solution of 2′,3′-*O*-isopropylidene-adenosine (300 mg, 1.0 mmol) and 4-*N*,*N*-dimethylaminopyridine (18 mg, 0.2 mmol) in pyridine (4 mL). After stirring for 4 h under argon, the solvent was evaporated in vacuo. Flash column chromatography (silica; MeOH–$CHCl_3$ 1:19) yielded the title compound as a white solid (460 mg, 86%), mp 144–146°C (lit.[5] 43–44°C); ^{1}H NMR (300 MHz, $CDCl_3$+MeOH-d_4, TMS, 25°C): δ (ppm) 8.24 (1H, s, Ar-*H* adenine), 8.21 (1H, s, Ar-*H* adenine), 7.58 and 7.43–7.31 (10H, m, Ph-*H*), 6.17 (1H, d, *J*=2.5 Hz, $H_{1'}$), 5.21 (1H, dd, *J*=6.1, 2.5 Hz, $H_{2'}$), 4.92 (1H, dd, *J*=6.1, 2.6 Hz, $H_{3'}$), 4.47 (1H, q, *J*=4.2, 2.5 Hz, $H_{4'}$), 3.98–3.65 (2H+MeOH, m, $H_{5'}$ and $H_{5''}$), 1.63 (3H, s, $-CH_3$), 1.39 (3H, s, $-CH_3$), 1.03 (9H, s, $(CH_3)_3C-$); MS (SIMS): *m/z*: 545 $[M]^+$, 487 [M−H−^{t}Bu]$^+$, 468 [M−Ph]$^+$. The product gave a single spot on TLC (chloroform–silica gel).

4.1.6. 2′,3′-*O*-Isopropylidene-5′-*O*-(2-methylpropyl)diphenylsilyl-guanosine (4). (2-Methylpropyl)diphenylchlorosilane (0.3 mL, 1.1 mmol) was added to a suspension of 2′,3′-*O*-isopropylidene-guanosine (300 mg, 0.9 mmol) and 4-*N*,*N*-dimethylaminopyridine (17 mg, 0.1 mmol) in pyridine (4 mL). After stirring for 4 h under argon, the solvent was evaporated in vacuo. Flash column chromatography (silica; MeOH–$CHCl_3$ 1:9) yielded the title compound as a white solid (499 mg, 96%). A small portion was recrystallized from ethanol. Mp 257–259°C; ^{1}H NMR (300 MHz, $CDCl_3$+MeOH-d_4, TMS, 25°C): δ (ppm) 7.71 (1H, s, Ar-*H* guanine) 7.64–7.58 (4H, m, Ph-*H*), 7.44–7.33 (6H, m, Ph-*H*), 5.95 (1H, d, *J*=2.7 Hz, $H_{1'}$), 5.15 (1H, dd, *J*=6.3, 2.7 Hz, $H_{2'}$), 4.91 (1H, dd, *J*=6.3, 3.0 Hz, $H_{3'}$), 4.36 (1H, q, *J*=4.8, 3.0 Hz, $H_{4'}$), 3.84 (2H, dAB, *J*=11.3, 4.8 Hz, $H_{5'}$), 1.61 (3H, s, $-CH_3$), 1.39 (3H, s, $-CH_3$), 1.04 (9H, s, $(CH_3)_3C$-). ^{13}C NMR (300 MHz, DMSO-d_6, TMS, 25°C): δ_C (ppm) 156.79 (q), 153.56 (q), 150.53 (q), 136.11 (+), 134.99 (+), 132.85 (q), 132.61 (q), 129.84 (+), 129.81 (+), 127.85 (+), 127.77 (+), 116.99 (q), 113.16 (q), 88.21 (+), 87.14 (+), 83.66 (+), 80.91 (+), 64.38 (−), 27.04 (+), 26.56 (+), 25.36 (+), 18.75 (q); MS (SIMS): *m/z*: 583 $[M-H+Na]^+$, 561 $[M]^+$, 485 $[M+H-Ph]^+$; elemental analysis calcd (%) for $C_{29}H_{35}N_5O_5Si$ (561.7): C 62.01, H 6.28, N 12.47; found C 61.88, H 6.41, N 12.40.

4.1.7. 2′,3′-*O*-Isopropylidene-5′-*O*-(2-methylpropyl)diphenylsilyl-uracil (5). 5′-*O*-(2-Methylpropyl)diphenylsilyl-uracil (500 mg, 1.0 mmol) and tosic acid monohydrate (3 mg, 15 μmol) were dissolved in DMF (2 mL). 2,2-Dimethoxypropane (0.25 mL, 2.1 mmol) was added to it and the mixture was left to stir overnight. Dowex 550A OH resin (100 mg) dispersed in methanol was added and subsequently filtered off. The filtrate was evaporated in vacuo. Flash column chromatography (silica; MeOH–$CHCl_3$ 5:95) yielded both starting material (215 mg, 0.4 mmol) and the title compound (217 mg, 40%). Mp 76–78°C (lit.[5] 67–68°C); ^{1}H NMR (300 MHz, $CDCl_3$, TMS, 25°C): δ (ppm) 8.59 (1H, s, N–*H*), 7.61 (5H, m, Ph-*H* and H_6), 7.41 (6H, m, Ph-*H*), 5.98 (1H, d, J=2.8 Hz, $H_{1'}$), 5.42 (1H, d, J=8.1 Hz, H_5), 4.82 (1H, dd, J=6.2, 3.3 Hz, $H_{2'}$), 4.73 (1H, dd, J=6.2, 2.8 Hz, $H_{3'}$), 4.27 (1H, q, J=3.1 Hz, $H_{4'}$), 4.00 (1H, dd, J=11.7, 2.6 Hz, $H_{5'}$), 3.84 (1H, dd, J=11.7, 3.5 Hz, $H_{5''}$), 1.58 (3H, s, –CH_3), 1.35 (3H, s, –CH_3), 1.08 (9H, s, (CH_3)$_3$C–); MS (SIMS): *m*/*z*: 523 $[MH]^+$, 465 $[M-{}^tBu]^+$, 445 $[M-Ph]^+$. The product gave a single spot on TLC (chloroform–silica gel).

4.1.8. 2′,3′-*O*-Isopropylidene-5′-*O*-(2-methylpropyl)diphenylsilyl-cytosine (6). (2-Methylpropyl)diphenylchlorosilane (0.44 mL, 1.9 mmol) was added to a solution of 2′,3′-*O*-isopropylidene-cytosine (500 mg, 1.6 mmol) and 4-*N*,*N*-dimethylaminopyridine (382 mg, 3.1 mmol) in pyridine (5 mL). After stirring for overnight under argon, the solvent was evaporated in vacuo. Traces of pyridine were removed by repeated evaporation from toluene. Flash column chromatography (silica; MeOH–$CHCl_3$ 1:9) yielded the title compound as a white solid (792 mg, 97%). Mp 125–128°C; ^{1}H NMR (300 MHz, $CDCl_3$, TMS, 25°C): δ (ppm) 9.54, 8.58 (2H, s, N–*H*), 7.70 (1H, d, J=7.5 Hz, H_5 or H_6), 7.62 and 7.41 (10H, m, Ph-*H*), 6.15 (1H, d, J=7.8 Hz, H_5 or H_6), 5.87 (1H, d, J=2.1 Hz, $H_{1'}$), 4.72 (2H, m, $H_{2'}$ and $H_{3'}$), 4.29 (1H, m, $H_{4'}$), 3.84 (2H, dd, J=11.7, 3.9 Hz, $H_{5'}$), 1.55 (3H, s, –CH_3), 1.32 (3H, s, –CH_3), 1.07 (9H, s, (CH_3)$_3$C–); MS (SIMS): *m*/*z*: 522 $[MH]^+$, 461 $[M-{}^tBu]^+$, 444 [M−Ph]; elemental analysis calcd (%) for $C_{28}H_{35}N_3O_5Si$ (521.7): C 64.46, H 6.76, N 8.05; found C 63.59, H 6.76, N 7.87.

4.1.9. 9-[4-(1,1-Dimethylethoxycarbonyl)aminobenzyl]-*N*6-(4-methoxybenzoyl)adenine (11). Sodium hydride (45 mg, 1.9 mmol) was added to a dispersion of *N*6-(4-methoxybenzoyl)adenine (506 mg, 1.9 mmol) in DMF (10 mL). After stirring for 20 min, the mixture was cooled and a solution of 4-(1,1-dimethylethoxycarbonyl)aminobenzylbromide (538 mg, 1.9 mmol) in DMF (10 mL) was added dropwise. After 3 h, methanol saturated with CO_2 (1 mL) was added and the solvent was subsequently evaporated in vacuo. Residual DMF was removed by repeated evaporation from toluene. Flash column chromatography (silica; MeOH–$CHCl_3$ 2:98) yielded the title compound as a yellow solid (231 mg, 26%). An analytically pure sample was obtained by recrystallisation from MeOH–H_2O 95:5, mp 115–117°C; ^{1}H NMR (300 MHz, DMSO-d_6, TMS, 25°C): δ (ppm) 8.77 (1H, s, *H*-2), 8.11 (1H, s, *H*-8), 8.07 (2H, d, J=9.0 Hz, Ar*H*), 7.41 (2H, d, J=8.7 Hz, Ar*H*), 7.27 (2H, d, J=9.0 Hz, Ar*H*), 7.01 (2H, d, J=9.0 Hz, Ar*H*), 5.40 (2H, s, CH_2), 3.90 (3H, s, OCH_3), 1.50 (9H, s, (CH_3)$_3$); MS (SIMS): *m*/*z*: 475 $[MH]^+$, 474 $[M]^+$; elemental analysis calcd (%) for $C_{25}H_{26}N_6O_4$ (474.5): C 63.28, H 5.52, N 17.71; found C 62.99, H 5.46, N 17.60.

4.1.10. 9-[4-Aminobenzyl]-*N*6-(4-methoxybenzoyl)adenine (12). 9-[4-(1,1-Dimethylethoxycarbonyl)aminobenzyl]-*N*6-(4-methoxybenzoyl)adenine (**11**) (225 mg, 0.5 mmol) was dissolved in 1,1,1-trifluoroacetic acid (3 mL) and stirred for 10 min. The solvent was evaporated in vacuo after which the residue was dissolved in CH_2Cl_2. This was washed with H_2O, basified with some $NaHCO_3$ (sat.). The aqueous layer was extracted twice with CH_2Cl_2 and the combined organic layers were dried over magnesium sulfate. The solvent was removed in vacuo, yielding the title compound (175 mg, 98%). An analytically pure sample was obtained by recrystallisation from MeOH–H_2O 4:1, mp 119–121°C; ^{1}H NMR (300 MHz, DMSO-d_6, TMS, 25°C): δ (ppm) 10.94 (1H, s, N*H*), 8.71 (1H, s, *H*-2), 8.49 (1H, s, *H*-8), 8.01 (2H, d, J=8.8 Hz, Ar*H*), 7.07 (4H, m, Ar*H*), 6.50 (2H, d, J=8.4 Hz, Ar*H*), 5.26 (2H, s, CH_2), 5.11 (2H, s, NH_2), 3.84 (3H, s, OCH_3); MS (SIMS): *m*/*z*: 376 $[M+2H]^+$, 375 $[M+H]^+$, 374 $[M]^+$; elemental analysis calcd (%) for $C_{20}H_{18}N_6O_2$ (374.4): C 64.16, H 4.85, N 22.45; found C 61.45, H 5.17, N 21.33.

4.1.11. 9-[4-(Cholesterylcarbonylamino)benzyl]-*N*6-(4-methoxybenzoyl)adenine (13). A solution of cholesteryl-chloroformate (270 mg, 0.6 mmol) in THF (3 mL) was added to a solution of 9-[4-aminobenzyl]-*N*6-(4-methoxybenzoyl)adenine (**12**) (150 mg, 0.4 mmol) and triethylamine (0.17 mL) in DMF (3 mL). The mixture was stirred at room temperature for 3 h. The solvent was evaporated in vacuo and residual DMF was removed by repeated evaporation from toluene. Flash column chromatography (silica; acetone–CH_2Cl_2 1:4) yielded the title compound as a white solid (138 mg, 44%). An analytically pure sample was obtained by recrystallisation from ethyl acetate–hexane, mp>230°C (decomp.); ^{1}H NMR (300 MHz, $CDCl_3$, TMS, 25°C): δ (ppm) 8.95 (1H, s, N*H*), 8.81 (1H, s, *H*-2), 7.99 (2H, d, J=8.8 Hz, Ar*H*), 7.94 (1H, s, *H*-8), 7.38 (2H, d, J=8.5 Hz, Ar*H*), 7.27 (2H, d, J=6.7 Hz, Ar*H*), 6.98 (2H, d, J=8.9 Hz, Ar*H*), 6.67 (1H, s, N*H*), 5.38 (3H, s, CH_2 and chol. *H*-6), 4.60 (1H, m, chol. OC*H*), 3.88 (3H, s, OCH_3), 2.39–2.32, 2.03–0.67 (43H, m, chol.-*H*); MS (SIMS): *m*/*z*: 786 $[M]^-$, 785 $[M-H]^-$, 784 $[M-2H]^-$, 268 [*N*6-(4-methoxybenzoyl)adenine]$^-$; elemental analysis calcd (%) for $C_{48}H_{62}N_6O_4$ (787.0): C 73.25, H 7.94, N 10.68; found C 72.69, H 8.09, N 11.04.

4.1.12. 1-[4-(Cholesterylcarbonylamino)benzyl]adenine (7). Ammonia (6 mL, 25% solution in water) was added to a solution of 1-[4-(cholesterylcarbonylamino)benzyl]-*N*6-(4-methoxybenzoyl)adenine (**13**) (200 mg, 0.3 mmol) in THF (12 mL). This was heated to 50°C for 7 days. The solvent was evaporated in vacuo, after which the residue was partitioned between $CHCl_3$ and H_2O. The organic layer was separated, the aqueous layer was extracted twice with $CHCl_3$ and the combined organic layers were dried over magnesium sulfate. The solvent was removed in vacuo. Flash column chromatography (silica; acetone–$CHCl_3$ 3:7) yielded the title compound as a white solid (140 mg, 84%). An analytically pure sample was obtained by recrystallisation from EtOH, mp 214–216°C; ^{1}H NMR (300 MHz,

$CDCl_3$, TMS, 25°C): δ (ppm) 8.39 (1H, s, *H*-2), 7.74 (1H, s, *H*-8), 7.37 (2H, d, *J*=8.4 Hz, Ar*H*), 7.25 (2H, d, overlap with chloroform signal, Ar*H*), 6.70 (1H, s, N*H*), 5.67 (2H, s, NH_2), 5.40 (1H, m, chol. *H*-6), 5.31 (2H, s, CH_2), 4.60 (1H, m, chol. OC*H*), 2.40–2.37, 1.99–0.68 (43H, m, chol.-*H*); MS (SIMS): *m/z*: 652 $[M]^-$, 651 $[M-H]^-$, 134 $[adenine]^-$; elemental analysis calcd (%) for $C_{40}H_{56}N_6O_2$ (652.9): C 73.58, H 8.65, N 12.87; found C 72.76, H 8.64, N 12.48.

4.1.13. 1-[4-(1,1-Dimethylethoxycarbonyl)aminobenzyl]-*N*4-(4-(1,1-dimethylethyl)benzoyl)cytosine (14). Sodium hydride (26 mg, 1.1 mmol) was added to a dispersion of *N*4-(4-(1,1-dimethylethyl)benzoyl)cytosine (269 mg, 1.0 mmol) in DMF (5 mL). After stirring for 20 min, a solution of 4-(1,1-dimethylethoxycarbonyl)aminobenzylbromide (340, 1.2 mmol) in DMF (5 mL) was added dropwise. After 3 h, methanol saturated with CO_2 (1 mL) was added and the solvent was subsequently evaporated in vacuo. Residual DMF was removed by repeated evaporation from toluene. Flash column chromatography (silica; MeOH–$CHCl_3$ 4:96) yielded the title compound as a white solid (451 mg, 96%). An analytically pure sample was obtained by recrystallisation from MeOH, mp>177°C (decomp.); ^{1}H NMR (300 MHz, DMSO-d_6, TMS, 25°C): δ (ppm) 11.07 (1H, s, N*H*), 9.34 (1H, s, N*H*), 8.23 (1H, d, *J*=6.9 Hz, *H*-6), 7.94 (2H, d, *J*=8.3 Hz, Ar-*H*), 7.51 (2H, d, *J*=8.3 Hz, Ar-*H*), 7.41 (2H, d, *J*=8.4 Hz, Ar-*H*), 7.31 (1H, d, *J*=7.0 Hz, *H*-5), 7.23 (2H, d, *J*=8.4 Hz, Ar*H*), 4.94 (2H, s, CH_2), 1.45 (9H, s, $(CH_3)_3$), 1.29 (9H, s, $(CH_3)_3$). MS (SIMS): *m/z*: 477 $[MH]^+$, 476 $[M]^+$, 272 $[M-CH_2C_6H_4NHBOC+2H]^+$, 206 $[CH_2C_6H_4NHBOC]^+$, 161 $[C(O)C_6H_4C(CH_3)_3]$; elemental analysis calcd (%) for $C_{27}H_{32}N_4O_4$ (476.6): C 68.05, H 6.77, N 11.76; found C 67.86, H 6.73, N 11.79.

4.1.14. 1-[4-Aminobenzyl]-*N*4-(4-(1,1-dimethylethyl)-benzoyl)cytosine (15). 1-[4-(1,1-Dimethylethoxycarbonyl)-aminobenzyl]-*N*4-(4-(1,1-dimethylethyl)benzoyl)cytosine (**14**) (395 mg, 0.8 mmol) was dissolved in 1,1,1-trifluoroacetic acid (2 mL) and stirred for 10 min. The solvent was removed in vacuo after which the residue was dissolved in CH_2Cl_2. This was washed with H_2O, basified with some $NaHCO_3$ (sat.). The aqueous layer was extracted twice with CH_2Cl_2 and the combined organic layers were dried over magnesium sulfate. The solvent was removed in vacuo, yielding the title compound (288 mg, 92%). An analytically pure sample was obtained by recrystallisation from MeOH–H_2O 4:1, mp 118–120°C; ^{1}H NMR (300 MHz, DMSO-d_6, TMS, 25°C): δ (ppm) 8.64 (1H, s, N*H*), 7.81 (2H, d, *J*=8.4 Hz, Ar*H*), 7.53 (4H, m, Ar*H*, *H*-5 and *H*-6), 7.14 (2H, d, *J*=7.5 Hz, Ar*H*), 6.67 (2H, d, *J*=6.5 Hz, Ar*H*), 4.97 (2H, s, CH_2), 3.76 (2H, s, NH_2), 1.34 (9H, s, $(CH_3)_3$); MS (SIMS): *m/z*: 378 $[M+2H]^+$, 377 $[MH]^+$, 376 $[M]^+$, 272 $[M-CH_2C_6H_4NH_2+2H]^+$, 161 $[C(O)C_6H_4C(CH_3)_3]^+$, 106 $[CH_2C_6H_4C(CH_3)_3]^+$; elemental analysis calcd (%) for $C_{25}H_{26}N_6O_4$ (474.5): C 63.28, H 5.52, N 17.71; found C 62.99, H 5.46, N 17.60.

4.1.15. 1-[4-(Cholesterylcarbonylamino)benzyl]-*N*4-(4-(1,1-dimethylethyl)benzoyl)cytosine (16). A solution of cholesterylchloroformate (658 mg, 1.5 mmol) in THF (10 mL) was added to a solution of 1-[4-aminobenzyl]-*N*4-(4-(1,1-dimethylethyl)benzoyl)cytosine (**15**) (460 mg, 1.2 mmol) and triethylamine (0.6 mL) in THF (10 mL) at 0°C. After 15 min the solution was allowed to reached room temperature and was left for 3 h. $CHCl_3$ and H_2O (100 mL each) were added, after which the organic layer was separated. The aqueous layer was extracted twice with $CHCl_3$ and the combined organic layers were dried over magnesium sulfate. The solvent was removed in vacuo. Flash column chromatography (silica; acetone–CH_2Cl_2 1:9) yielded the title compound as a white solid (578 mg, 60%)). An analytically pure sample was obtained by recrystallisation from MeOH, mp 230–232°C; ^{1}H NMR (300 MHz, $CDCl_3$, TMS, 25°C): δ (ppm) 8.70 (1H, s, N*H*), 7.81 (2H, d, *J*=8.4 Hz, Ar*H*), 7.58 (1H, d, *J*=7.2 Hz, *H*-5 or *H*-6), 7.51 (3H, d, Ar*H* and *H*-5 or *H*-6), 7.40 (2H, d, *J*=8.5 Hz, Ar*H*), 7.29 (2H, d, *J*=8.6 Hz, Ar*H*), 6.75 (1H, s, N*H*), 5.40 (1H, m, chol. *H*-6), 5.04 (2H, s, CH_2), 4.59 (1H, m, chol. OC*H*), 2.40–2.38, 1.99–0.85, 0.68 (43H, m, chol.-*H*), 1.33 (9H, s, $C(CH_3)$); MS (SIMS): *m/z*: 788 $[M]^-$, 787 $[M-H]^-$, 786 $[M-2H]^-$, 270 [*N*4-(4-(1,1-dimethylethyl)-benzoyl)cytosine]$^-$; elemental analysis calcd (%) for $C_{50}H_{68}N_4O_4$ (789.1): C 76.10, H 8.69, N 7.10; found C 75.51, H 8.63, N 7.08.

4.1.16. 1-[4-(Cholesterylcarbonylamino)benzyl]cytosine (8). Ammonia (3 mL, 25% solution in water) was added to a solution of 1-[4-(cholesterylcarbonylamino)benzyl]-*N*4-(4-(1,1-dimethylethyl)benzoyl)cytosine (**16**) (187 mg, 0.2 mmol) in THF (6 mL). This was heated to 50°C for 7 days. The solvent was evaporated in vacuo, after which the residue was partitioned between $CHCl_3$ and H_2O. The organic layer was separated, the aqueous layer was extracted twice with $CHCl_3$ and the combined organic layers were dried over magnesium sulfate. The solvent was removed in vacuo. Flash column chromatography (silica; MeOH–$CHCl_3$ 1:19) yielded the title compound as a white solid (129 mg, 87%). Also starting material (15 mg, 8%) was isolated. An analytically pure sample was obtained by recrystallisation from EtOH, mp 257–259°C; ^{1}H NMR (300 MHz, $CDCl_3$+MeOH-d_4, TMS, 25°C): δ (ppm) 7.39 (2H, d, Ar*H*), 7.26 (1H, d, *J*=7.2 Hz, *H*-6), 7.21 (2H, d, Ar*H*), 5.74 (1H, d, *J*=7.2 Hz, *H*-5), 5.40 (1H, m, chol. *H*-6), 4.89 (2H, s, CH_2), 4.56 (1H, m, chol. OC*H*), 2.41–2.35, 2.00–1.87, 1.57–0.69 (43H, m, chol.-*H*); MS (SIMS): *m/z*: 628 $[M]^-$, 627 $[M-H]^-$, 199 [benzzylcytosine$-H]^-$, 110 $[cytosine]^-$; elemental analysis calcd (%) for $C_{39}H_{56}N_4O_3$ (628.9): C 74.48, H 8.98, N 8.91; found C 73.59, H 8.88, N 8.69.

4.2. Measurements of sol–gel transition temperatures

The sealed tube containing the gel was immersed inversely in a thermostated oil bath. The temperature was raised at a rate of 1°C min^{-1}. Here, the T_{gel} was defined as the temperature at which the gel turned into the sol phase.

4.3. CD and UV measurements

Variable temperature CD and UV measurements were carried out with a JASCO J-720 spectrometer and a JASCO V-570 spectrometer, respectively, using a 0.1 mm cell with a water jacket. Generally, the gelation with **1** took a relatively long time, so that the sample in the cell was aged for 12 h before measurements.

4.4. SEM observations

A Hitachi S-900S scanning electron microscope was used for taking the SEM pictures. The gel was prepared in a sample tube and frozen by liquid nitrogen. The frozen specimen was evaporated by a vacuum pump for 1 day. The dry sample obtained was shielded with platin. The accelerating voltage of SEM was 12.0 kV and the emission current was 10 μA.

Acknowledgements

We thank Professor D. N. Reinhoudt (Twente University) for his useful comments and continuous encouragement made through Chemotransfiguration Project.

References

1. (a) Terech, P.; Weiss, R. G. *Chem. Rev.* **1997**, *97*, 3133–3159. (b) van Esch, J.; Schoonbeek, F.; de Loos, M.; Veen, E. M.; Kellogg, R. M.; Feringa, B. L. *Nato ASI Ser. C* **1999**, *527*, 233–259. (c) Gronwald, O.; Snip, E.; Shinkai, S. *Curr. Opin. Coll. Int. Sci.* **2002**, *7*, 148–156. (d) van Esch, J. H.; Feringa, B. L. *Angew. Chem., Int. Ed.* **2000**, *39*, 2263–2266.
2. (a) Hanabusa, K.; Maesaka, Y.; Kimura, M.; Shirai, H. *Tetrahedron Lett.* **1999**, *40*, 2385–2388. (b) Suzuki, M.; Yumoto, M.; Kimura, M.; Shirai, H.; Hanabusa, K. *Chem. Commun.* **2002**, 884–885. (c) Hanabusa, K.; Maesaka, Y.; Suzuki, M.; Kimura, M.; Shirai, H. *Chem. Lett.* **2000**, 1168–1169. (d) van Esch, J.; Schoonbeek, F.; de Loos, M.; Kooijman, H.; Spek, A. L.; Kellogg, R. M.; Feringa, B. L. *Chem. Eur. J.* **1999**, *5*, 937–958. (e) Shi, C.; Huang, Z.; Kilic, S.; Xu, J.; Enick, R. M.; Beckman, E. J.; Carr, A. J.; Melendez, R. E.; Hamiltion, A. D. *Science* **1999**, *286*, 1540–1543.
3. (a) Gronwald, O.; Shinkai, S. *Chem. Eur. J.* **2001**, *7*, 4328–4334. (b) Yoza, K.; Amanokura, N.; Ono, Y.; Akao, T.; Shinmori, H.; Takeuchi, M.; Shinkai, S.; Reinhoudt, D. N. *Chem. Eur. J.* **1999**, *5*, 2722–2729. (c) Hamachi, I.; Kiyonaka, S.; Shinkai, S. *Tetrahedron Lett.* **2001**, *42*, 6141–6145. (d) Shimizu, T.; Masuda, M. *J. Am. Chem. Soc.* **1997**, *119*, 2812–2818. (e) Hafkamp, R. J. H.; Feiters, M. C.; Nolte, R. J. M. *J. Org. Chem.* **1999**, *64*, 412–426.
4. (a) Murata, K.; Aoki, M.; Suzuki, T.; Harada, T.; Kawabata, H.; Komori, T.; Ohseto, F.; Ueda, K.; Shinkai, S. *J. Am. Chem. Soc.* **2000**, *116*, 6664–6676. (b) Jung, J. H.; Ono, Y.; Shinkai, S. *Tetrahedron Lett.* **1999**, *40*, 8395–8399. (c) Jung, J. H.; Ono, Y.; Shinkai, S. *J. Chem. Soc., Perkin Trans. 2* **1999**, 1289–1291. (d) Jung, J. H.; Ono, Y.; Shinkai, S. *Angew. Chem., Int. Ed.* **2000**, *39*, 1862–1865. (e) Jung, J. H.; Ono, Y.; Shinkai, S. *Langmuir* **2000**, *16*, 1643–1649. (f) Jung, J. H.; Ono, Y.; Sakurai, K.; Sano, M.; Shinkai, S. *J. Am. Chem. Soc.* **2000**, *122*, 8648–8653. (g) Amaike, M.; Kobayashi, H.; Shinkai, S. *Bull. Chem. Soc. Jpn* **2000**, *73*, 2553–2558. (h) Jung, J. H.; Kobayashi, H.; Masuda, M.; Shimizu, T.; Shinkai, S. *J. Am. Chem. Soc.* **2001**, *123*, 8785–8789. (i) Wang, R.; Geiger, C.; Chen, L.; Swanson, B.; Whitten, D. G. *J. Am. Chem. Soc.* **2000**, *122*, 2399–2400.
5. (a) Amaike, M.; Kobayashi, H.; Shinkai, S. *Chem. Lett.* **2001**, 620–621. (b) Mizoshita, N.; Monobe, H.; Inoue, M.; Ukon, M.; Watanabe, T.; Shimizu, Y.; Hanabusa, K.; Kato, T. *Chem. Commun.* **2002**, 428–429. (c) Kobayashi, H.; Friggeri, A.; Koumoto, K.; Amaike, M.; Shinkai, S.; Reinhoudt, D. N. *Org. Lett.* **2002**, *4*, 1423–1426.
6. Maitra, U.; Kumar, P. V.; Chandra, N.; Souza, L. J. D.; Prasanna, M. D.; Raju, A. R. *Chem. Commun.* **1999**, 595–596.
7. Sohna, J.-E. S.; Fages, F. *Chem. Commun.* **1997**, 327–328.
8. Amanokura, N.; Kanekiyo, Y.; Shinkai, S.; Reinhoudt, D. N. *J. Chem. Soc., Perkin Trans. 2* **1999**, 1995–2000.
9. Kobayashi, H.; Amaike, M.; Jung, J. H.; Friggeri, A.; Shinkai, S.; Reinhoudt, D. N. *Chem. Commun.* **2001**, 1038–1039.
10. For hydrogen-bonding additives see (a) Jeong, S.; Murata, K.; Shinkai, S. *Supramol. Sci.* **1996**, *3*, 83–86. (b) Tamaru, S.; Luboradzki, R.; Shinkai, S. *Chem. Lett.* **2001**, 336–337. (c) Tamaru, S.; Uchino, S.; Takeuchi, M.; Ikeda, M.; Hatano, T.; Shinkai, S. *Tetrahedron Lett.* **2002**, *43*, 3751–3755.
11. Preliminary communication: Snip, E.; Shinkai, S.; Reinhoudt, D. N. *Tetrahedron Lett.* **2001**, *42*, 2153–2156.
12. Robins, J. M.; Hatfield, P. W. *Can. J. Chem.* **1982**, *60*, 547–553.
13. Bellamy, F. D.; Ou, K. *Tetrahedron Lett.* **1984**, *25*, 839–842.
14. Hanessian, S.; Lavallee, P. *Can. J. Chem.* **1975**, *25*, 2975–2977.
15. Will, D. W.; Breipohl, G.; Langner, D.; Knolle, J.; Uhlmann, E. *Tetrahedron* **1995**, *51*, 12069–12082.
16. (a) Thrierr, J. C.; Dourlent, M.; Leng, M. *J. Mol. Biol.* **1971**, *58*, 815–830. (b) Bode, D.; Heinecke, M.; Scherna, U. *Biochem. Biophys. Res. Commun.* **1973**, *52*, 1234–1240.
17. Inoue, K.; Ono, Y.; Kanekiyo, T.; Ishi-I, T.; Yoshihara, K.; Shinkai, S. *J. Org. Chem.* **1999**, *64*, 2933–2937.
18. The CD spectra were measured under the following conditions: [poly(U)]=2.40×10^{-4} mol dm^{-3}, [poly(A/U)]=1.15×10^{-4} mol dm^{-3}/1.20×10^{-4} mol dm^{-3}, 5°C, [NaCl]=10 mmol dm^{-3}.
19. Miles, T.; Frazier, J. *Biochem. Biophys. Res. Commun.* **1964**, *14*, 21–28.